



# Investigation of the effects of drill geometry on drilling performance and hole quality

Mehtap Yavuz<sup>1</sup> · Hüseyin Gökçe<sup>2</sup> · İbrahim Çiftçi<sup>3</sup> · Harun Gökçe<sup>4</sup> · Çağlar Yavaş<sup>5</sup> · Ulvi Şeker<sup>6</sup>

Received: 21 May 2019 / Accepted: 16 December 2019 / Published online: 23 January 2020  
© Springer-Verlag London Ltd., part of Springer Nature 2019

## Abstract

In this study, the effects of drill geometry on cutting performance and hole quality in the drilling process were investigated. Two newly developed drill geometries were compared with two commercially available drill geometries. In the drilling tests on GGG50 cast iron, 4 different drills, 4 different cutting speeds and 4 different feed rates were used for L16 experimental design. The drilling tests were performed with and without cutting fluid. The results were evaluated using the axiomatic design method, one of the multi-criteria decision making methods, in terms of thrust force, surface roughness, deviation on hole diameter and length of adhering workpiece material around the chisel edges. From the obtained results, it was seen that the best results were obtained from one of the newly developed drill geometries. In addition, wear test was carried out without cutting fluid using the drill which performed best. With this best performed drill, after 100 drilling operations in wet and dry conditions and after 1500 drilling operations in dry conditions, SEM images were taken from the used drills. After drilling 100 holes both in dry and wet drilling conditions, there was almost no wear on the drills. However, some adhered workpiece material was seen on the drills. In addition, the amount of adhered workpiece significantly increased in dry drilling condition.

**Keywords** Drilling · Drill geometry · GGG50

## 1 Introduction

Although various cutting tools are available for hole making, the twist drill is by far the most common one [1]. The various angles on a drill have been developed through experience over years. The drills are designed to produce accurate holes and to have high wear resistance. Small changes in drill geometry greatly influence the performance of the drill [2]. Therefore, the complex drill geometry incorporates numerous conflicts of

design objectives such as low drilling force and torque, high wear resistance, high torsional and bending strength and easy chip evacuation capability. Meeting these requirements necessitates the drill designer with a high level of experience [3].

When compared with the other material removal processes, the drilling process has quite a wide application field. Especially in the aerospace industry, drilling constitutes a large portion of the machining processes, up to 40–60% [4]. Therefore, optimisation of drill geometry is of great importance

✉ Mehtap Yavuz  
mehtapyavuz@karatekin.edu.tr

Hüseyin Gökçe  
huseyingokce@karatekin.edu.tr

İbrahim Çiftçi  
iciftci@karatekin.edu.tr

Harun Gökçe  
harungokce@yahoo.ca

Çağlar Yavaş  
c.yavas@karcan.com

Ulvi Şeker  
useker@gazi.edu.tr

<sup>1</sup> Department of Mechatronics, Çankırı Karatekin University, Çankırı, Turkey

<sup>2</sup> Department of Machinery, Çankırı Karatekin University, Çankırı, Turkey

<sup>3</sup> Department of Mechanical Engineering, Çankırı Karatekin University, Çankırı, Turkey

<sup>4</sup> Defense Industries Research and Development Institute, TÜBİTAK, Ankara, Turkey

<sup>5</sup> Product Development Department, Karcan Cutting Tools, Eskişehir, Turkey

<sup>6</sup> Department of Manufacturing Engineering, Gazi University, Ankara, Turkey

in order to improve drilled hole quality and decrease cost as small changes in the drill geometry greatly influences the drilling performance. Optimisation of twist drill geometries in drilling operations was investigated by many researchers.

Tsai and Wu developed a mathematical model taking into account drill point design and grinding parameters. Their model was capable of describing the drill point geometry for the conical, hyperboloidal and ellipsoidal drills. The model developed also enabled one to precisely predict and control the drill point geometry and the grinding parameters [5]. In another study, Tsai and Wu used computer to analyse drill point geometry accurately and conveniently [6].

Chen et al. developed a modified force model incorporating the splitting parameters for predicting the thrust forces and torque of a split-point drill. The effect of the notch angle on the thrust forces and torque was deduced. Drilling tests were also carried out on JIS 45C steel in order to compare the calculated and experimental thrust forces and torque. The optimisation of the drill point geometry was obtained by minimising the thrust forces and torque [7].

Ren and Ni examined the analysis of both flute and flank surface models and the evaluation of drill cutting edge angles. In their study, a mathematical model for the drill flute surface was developed by sweeping the polynomial representation of the flute cross-sectional curve. On the basis of the quadratic flank surface, a relationship between the grinding and the geometrical design parameters of the flank surface was also established. The analytical results matched well with the measured cutting angles for an example drill [8].

Paul et al. described a methodology to obtain the optimum shape for the chisel edge and cutting lips of drills to minimise thrust force and torque in drilling. A point geometry model based on the drill grinding parameters was used to ensure manufacturability of the optimised geometry. Three commonly used drill point geometries were optimised for drilling forces. A significant reduction was obtained in the drilling forces from the optimised drills [9].

Hsieh proposed a comprehensive and straightforward method for the design and analysis of helical micro-drills. This model described the relationship between the helical micro-drill point geometry and the grinding parameters. The proposed model was capable of describing a wide range of helical drills. The presented methodology facilitated the production of helical drills on a 6-axis CNC grinding machine [10].

Pirtini and Lazoglu developed a mathematical model based on the mechanics and dynamics of the drilling process for the prediction of cutting forces and hole quality. Their model was able to simulate the cutting forces for various cutting conditions in the process planning stage. In order to obtain drilled hole profiles in addition to cutting force prediction, measured frequency response functions of the spindle and tool system were integrated into the model. Therefore, the model allowed the determination and visualisation of drilled hole profiles in

3D. The outputs of the theoretical model were compared with those of dynamometer and CMM measurements. It was observed that they agree reasonably well [11].

Degenhardt et al. investigated the effect of groove-type chip breaker on drilling for different drill diameter and flute shapes. They proposed a generalised formulation to place chip breaker grooves on drills of varying diameter. Grooves were placed on the drill rake face of 6.35- and 3.18-mm diameter drills of standard and parabolic flute shapes. Validation experiments were carried out and the results indicated that chip size was reduced [12]. Audy presented the results of a computer-assisted study focusing on determining the relationship between the drill point geometry and the drill performance. The performance measures were forces and power in drilling [13, 14].

Wang and Zang carried out a study using drills with a modified drill point design with plane rake faced in order to reduce the drilling force and torque for drilling steels of high tensile strength. They carried out drilling experiments on a high tensile strength steel using these drills of modified point design. It was reported these drills not only reduced the thrust force and torque significantly but also improved the tool life [15]. In the second part of their study, they developed predictive models mathematically for the drilling forces, torque and power using the plane rake faced drills [16].

Sambhav et al. presented a method for modelling geometry and forces of twist drills with standard tip geometry. This model was capable of modelling any kind of drill point profile and of calculating the thrust force and torque mechanistically [17]. Ema investigated the impacts of the drill point geometry on cutting performance of the twist drills. Many drills with different web thicknesses, point angles, lip relief angles, helix angles and margin lengths were used, and torque and thrust force in drilling were measured. Torque significantly increased with the web thickness and the margin length and conversely decreased with the helix angle. There is an optimum point angle to minimize torque. Thrust force significantly increased with the web thickness and the relief angle and conversely decreased with the point angle and the helix angle [18].

Chatterjee et al. carried out a study to analyse the effect of various drilling parameters such as spindle speed, feed rate and drill bit diameter on performance characteristics such as thrust force, torque and circularity at entry and exit of the holes in drilling of titanium alloy using coated drill. In the study they conducted, they developed a machining model based on the Lagrangian approach using Deform-3D software. The performance characteristics obtained through the model was compared with the experimental results. Both results were closely agreed [19].

From the detailed literature review above, it is seen that considerable studies were carried out on the drill point design. These studies are mostly on various modelling techniques. In this study, the influence of different drill geometries was investigated experimentally. The effect of various drill point

designs and drilling parameters on the thrust force, surface roughness, deviation on hole diameter and length of adhering workpiece material around the cutting edges in drilling GGG50 workpiece was investigated. Four different drill geometries were tested. Two of them were commercially available while the other two were specially designed and produced within the scope of this study. The experimental results were optimised through the axiomatic design method.

## 2 Material and method

### 2.1 Workpiece and cutting tools

GGG50 cast iron blocks in dimensions of  $30 \times 140 \times 140$  mm were used as the workpiece material. Chemical composition of the workpiece is given in Table 1, while Table 2 gives some of its properties. Hardness value of this material was determined using a Brinell hardness tester. Three measurements were made and the average hardness value was found to be 193 HB. Microstructure of the workpiece is given in Fig. 1. Figure 1 shows that the microstructure is ferritic.

Four different two-flute solid carbide twist drills with internal cooling holes and 10 mm in diameter (Fig. 2) were used. Geometrical features of the drills are given in Fig. 2. These drills were denoted as drill 1, drill 2, drill 3 and drill 4. Drill 1 and drill 2 were commercially available drills, while drill 3 and drill 4 were specially produced by Karcan. Drill 1 and drill 2 were produced by Sandvik Coromant and Kennametal, respectively. Drill 1, drill 2, drill 3 and drill 4 had R846 Sandvik designation, KC7315 Kennametal designation, NG7 and NG6 Karcan designations, respectively.

Unlike drill 3, drill 4 had two clearance angles to increase cutting edge strength. In addition, two clearance angles also reduce the friction when the drill moves on the workpiece. The split angle of drill 4 was increased to  $43^\circ$ . This was considered to enable easy chip formation. Moreover, web thickness value of drill 4 was reduced to 2.6 mm to provide a larger chip evacuation channels.

### 2.2 Test equipment and devices

The experiments were designed using L16 orthogonal array (four levels and three factors). Minitab 16 was used for the experimental design. The drill geometry, cutting speed and feed rate were selected as the control factor. Table 3 gives the control factors and their levels.

**Table 2** Some properties of GGG50 cast iron [20]

Grade	Tensile strength (MPa)	Yield strength (MPa)	Elongation (%)
GGG 50	490.3	352.8	7

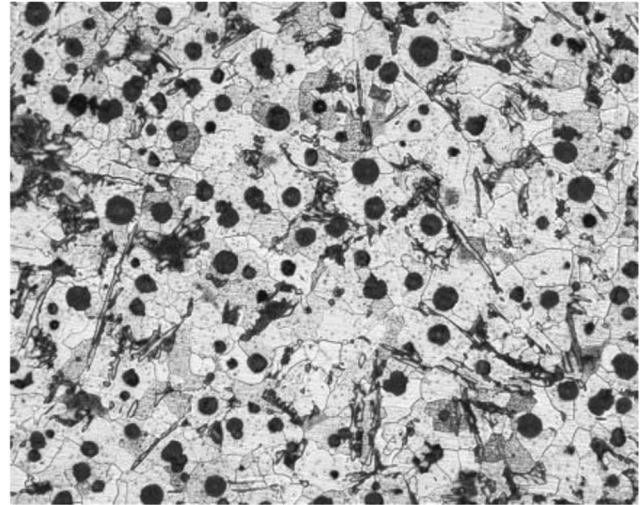


**Fig. 1** Microstructure of GGG50 ( $\times 100$ )

The drilling tests were carried out on a Johnford VMC-550 CNC vertical machining centre with Fanuc control unit. In order to enable the internal cooling through the drills, a GISS SC-16 spindle speeder was used. Components of the experimental setup used to measure the thrust force are presented in Fig. 3. At each cutting condition determined based on the L16 orthogonal array, 100 holes were drilled using cutting fluid. The values of thrust force, surface roughness, deviation on hole diameter and length of adhering workpiece material around the cutting edges were measured during and after drilling 100 holes.

For the measurement of the thrust force a KISTLER 9257-B dynamometer and an associated KISTLER 5070 amplifier was used. Surface roughness measurements were performed using a Mahr Perthometer M1 unit with a cutoff length of 0.8 mm and sampling length of 5.6 mm. For each hole, 3 surface roughness measurements were carried out (each at  $120^\circ$  angle apart) and the results were averaged. Deviation on hole diameter measurements of the holes was made with Hexagon Global Performance CMM device. For each hole, three deviation values were measured from three different

**Table 1** Chemical composition of GGG50 cast iron material (wt.%)

C	Si	Mn	P	S	Mg	Cr	Ni	Mo	Cu	Fe
5.4	2027	0.110	0.047	0.046	0.134	0.01	0.023	0.01	0.054	Balance

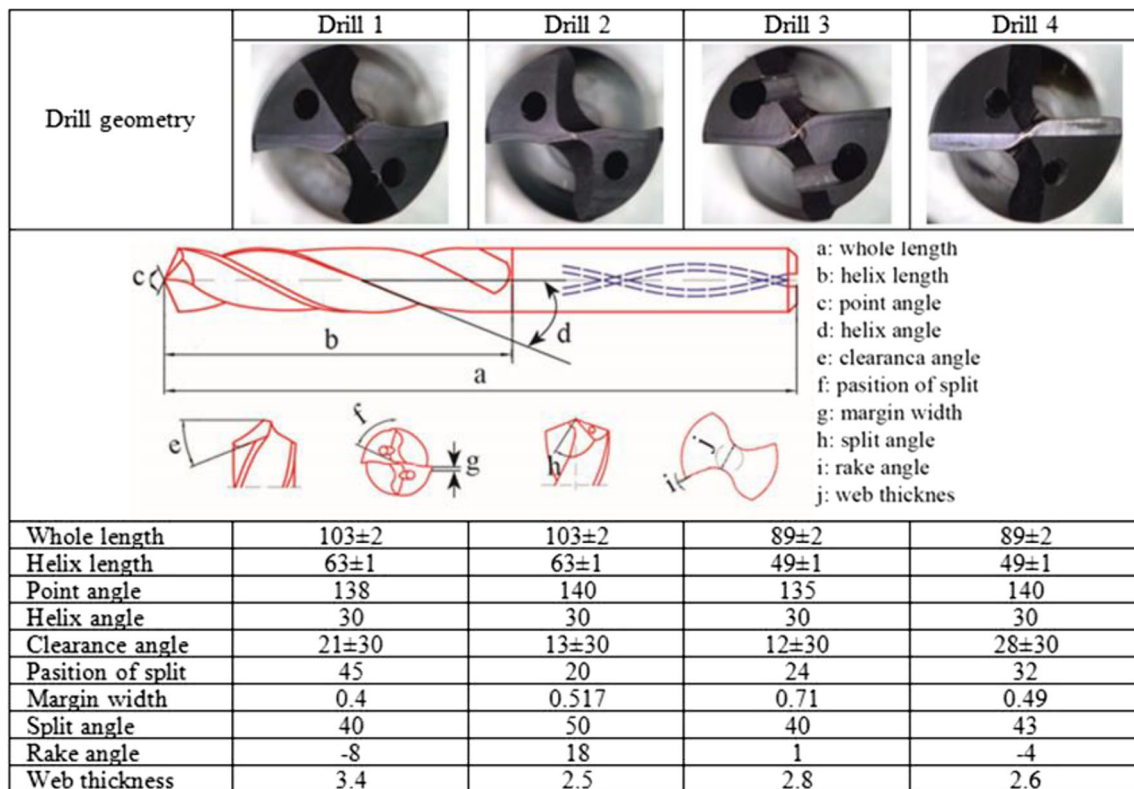


Fig. 2 Geometries of the drills

depths along the hole axis (5-, 15- and 25-mm depths). The used drill bits were examined under a Nikon SMZ800N stereo microscope capable of capturing images. Length of adhering workpiece on the web of drill was determined using AutoCAD software. In addition, a Carl Zeiss Ultra Plus Gemini FESEM scanning electron microscope (SEM) was used to examine the used drill 4 in detail and to carry out EDX analyses. The temperature measurements were made with the Fluke Ti200 instrument in dry condition during the wear test. The assumed emissivity of the measured material is 0.95. Position of the temperature measurement unit is shown in Fig. 3. The temperature in the drill bit was measured throughout a hole drilling cycle. The highest recorded temperature was taken into account for each measurement. Figure 4 gives a snapshot from the video file recorded during the temperature measurement.

Table 3 Control factors and their levels

Control factors	Unit	Levels			
		1	2	3	4
Drill geometry	–	Drill 1	Drill 2	Drill 3	Drill 4
Cutting speed	m/min	90	100	110	120
Feed rate	mm/rev	0.15	0.20	0.25	0.30

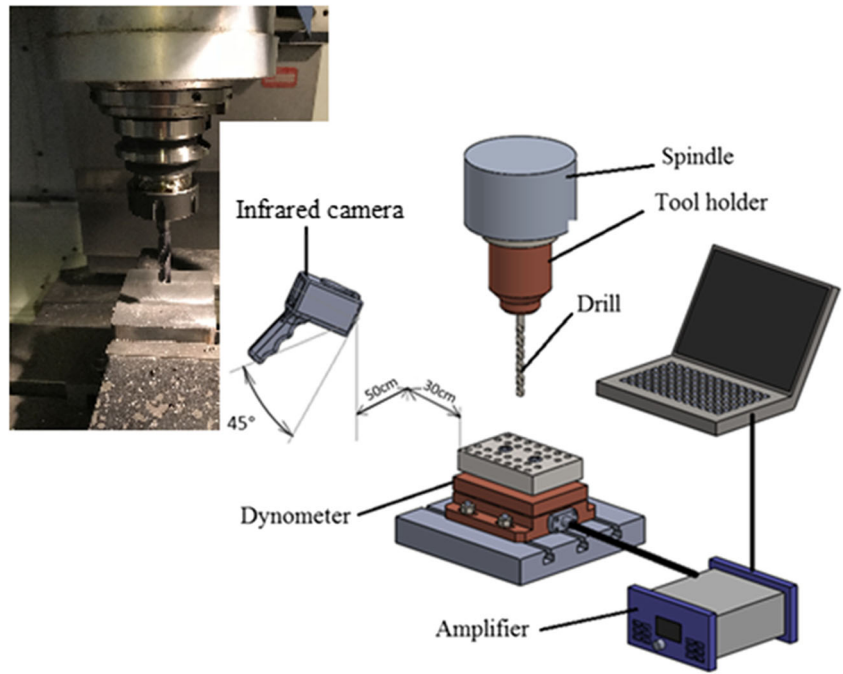
Having drilled 100 holes using cutting fluid, no significant wear was observed on the drills. Further drill wear test was carried out using drill 4 as it performed best in terms of surface roughness, deviation on hole diameter, thrust force and adhering workpiece material. Taksan TMC-500V CNC vertical machining centre was used for the wear test. In order to increase wear rate, the wear test was carried out without cutting fluid at 120 m/min cutting speed and 0.15 mm/rev feed rate. At these conditions, 1500 holes were drilled.

### 2.3 Axiomatic design method

Axiomatic design (AD) is a method developed by Suh to make the design of systems, processes and products more scientific. In this method, the independence axiom is used to create product designs, and the information axiom is used to select the best solution. In axiomatic design, the aim is to minimize the information content. In this study, information content of axiomatic design is used. The best choice for optimum drill geometry and cutting parameters is the smallest selection of the total information content.

Numerical values are needed to calculate the information content. In this study, the functional requirements needed for drilling are the thrust force, surface roughness, deviation on hole diameter and the adhering workpiece material, and these values will be used to calculate the information content. These values are certain values and there are no ranges. Therefore,

Fig. 3 Experimental setup



satisfaction charts, also defined by Nakazawa, are set to calculate the information contents of all alternatives for each functional requirement. Abscissa of the chart is for the functional requirement and the ordinate is for satisfaction level. Satisfaction degrees change from zero to one [21].

Taguchi’s quality measure (given in Eq. (1)) is used to calculate the information content.  $M_s$  is the degree of satisfaction of the system,  $m_d$  is the target value which is taken 1 in Eq. (1). The system variance ( $\sigma_s = 0$ ) is taken zero because of the certain values of systems. The coefficient  $C$  in the equation is the same as the significance levels of all alternatives and can be taken as 1.

$$J_L = C \cdot [\sigma_s^2 + (m_s - m_d)^2] \tag{1}$$

The performance criteria used in drilling, such as thrust force, surface roughness, deviation on hole diameter and adhering workpiece are all examples of the smaller-the-better type. For example, as a smaller-the-better type, satisfaction of thrust force is given below in Fig. 5, 951 N is the lowest thrust force among all alternatives and  $m_s$  will be 1, since the lowest thrust force is preferred in drilling operation. The most highest thrust force is 2418 N so that  $m_s$  will be 0.

In Suh’s original information axiom technique, the information content corresponding to each FR is simply summed up with all other terms without a weighting factor. The alternative that has the information ( $I$ ) is the best design. For each functional requirement, the satisfaction degrees and their information content of all alternatives and are calculated.

Fig. 4 A snapshot for the temperature measurement



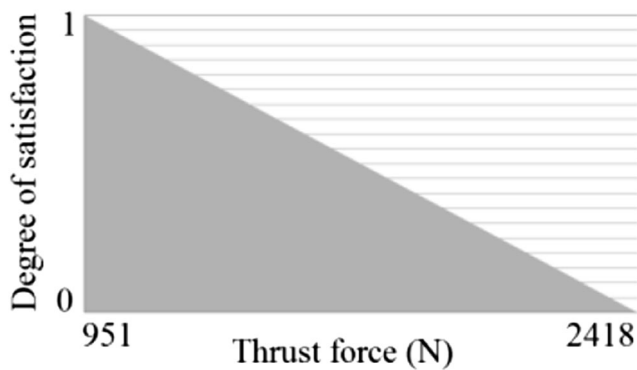


Fig. 5 Degree of satisfaction for thrust force

### 3 Results and discussion

#### 3.1 Thrust force, surface roughness, deviation on hole diameter and length of adhering workpiece

The thrust force, average surface roughness, deviation on hole diameter and length of adhering workpiece achieved as the response variables in drilling of GGG50 workpiece were measured during and after the drilling tests performed according to the L16 array. The lowest values of these response variables considerably improve the quality of the drilled hole. In Table 4, the values of the response variables are given against the control factors of the drill bit geometry, feed rate and cutting speed. The values in Table 4 were obtained after drilling 100 holes.

The cutting forces are based on three components of the cutting forces. The cutting force of the drill ( $F_c$ ) acting on a

shear lip is expressed by the thrust force ( $F_t$ ) and the radial force ( $F_r$ ). Due to the positions of the cutting lip of the drill, the radial forces generated in each of the cutting lip compensate each other. Therefore, in drilling operations,  $F_t$  and  $F_c$  forces have an effect. In general, the main cutting force is the largest of these three components. In drilling with drills, the greatest force is the thrust ( $F_t$ ) perpendicular to the surface being machined and in the Z direction.

When Table 4 is examined, it is seen that the thrust force ranges between 951 and 2418 N, that the average surface roughness ranges between 0.963 and 1.976  $\mu\text{m}$ , that the deviation on hole diameter ranges between 0.009 and 0.074 mm and that the length of adhering workpiece ranges between 0.192 and 1.254 mm. As the used drill bits are capable of drilling the holes having ISO roughness grade numbers of N6–N9 (equivalent to 0.8–6.3  $\mu\text{m}$ ), the obtained results fall within this range.

For a hole of 10-mm diameter, at the international dimension tolerance standards, hole tolerance H9 (0–0.043 mm) was determined and this tolerance range was used as the deviation range from the diameter. When the deviation on hole diameter values are examined, it is seen that these tolerances are exceeded in drilling with drill 1 (tests 2 and 4) and drill 3 (test 11). According to these results, the smallest thrust force, surface roughness and length of adhering workpiece values are obtained with drill 4, while the smallest deviation on hole diameter is obtained with drill 2.

The effect of the drill geometry, feed rate and cutting speed interactions on the thrust force is shown in Fig. 6. Figure 6 shows that the thrust force is influenced by changes in drill

Table 4 Experimental results

Test number	Control factors' codes	Drill bit geometry (A) Unit	Feed rate (B) mm/dev	Cutting speed (C) m/dak	Thrust force N	Average surface roughness $\mu\text{m}$	Deviation on hole diameter mm	Length of adhering workpiece mm
1	A1B1C1	Drill 1	0.15	90	1149	1.122	0.019	0.311
2	A1B2C2	Drill 1	0.2	100	1402	1.448	0.074	0.527
3	A1B3C3	Drill 1	0.25	110	1504	1.447	0.026	0.741
4	A1B4C4	Drill 1	0.3	120	1667	1.798	0.060	0.943
5	A2B1C2	Drill 2	0.15	100	1054	1.800	0.009	0.332
6	A2B2C1	Drill 2	0.2	90	1273	1.889	0.026	0.573
7	A2B3C4	Drill 2	0.25	120	1367	1.616	0.031	0.617
8	A2B4C3	Drill 2	0.3	110	1530	1.616	0.034	0.721
9	A3B1C3	Drill 3	0.15	110	1353	1.612	0.021	0.630
10	A3B2C4	Drill 3	0.2	120	1752	1.896	0.032	0.915
11	A3B3C1	Drill 3	0.25	90	2177	1.771	0.045	1.254
12	A3B4C2	Drill 3	0.3	100	2418	1.909	0.028	1.140
13*	A4B1C4	Drill 4	0.15	120	951	0.963	0.021	0.192
14	A4B2C3	Drill 4	0.2	110	1108	1.363	0.023	0.333
15	A4B3C2	Drill 4	0.25	100	1323	1.509	0.028	0.418
16	A4B4C1	Drill 4	0.3	90	1542	1.976	0.017	0.524

\* Optimal test conditions based on the axiomatic design criteria

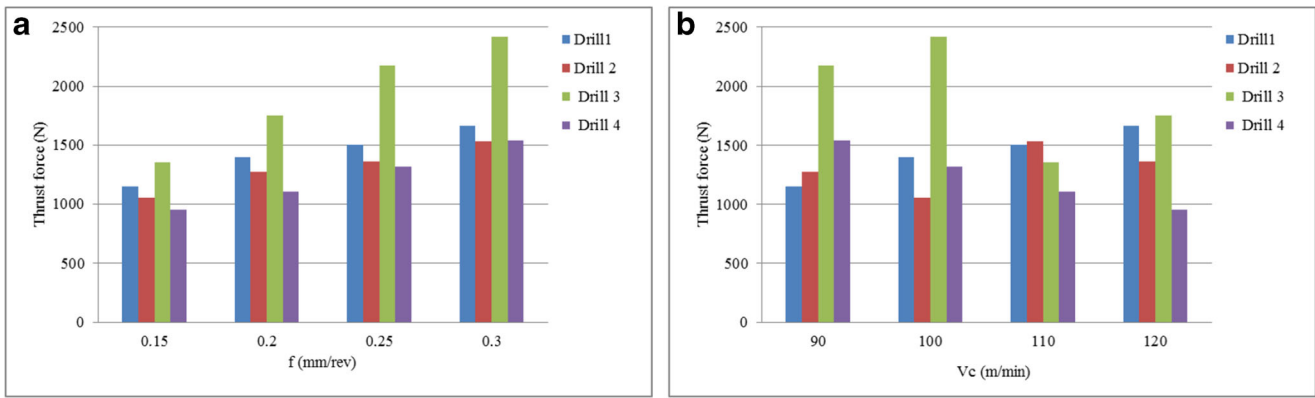


Fig. 6 Effect of a drill geometry-feed rate and b drill geometry-cutting speed interactions on the thrust force

geometry and feed rate. It is observed that there is an increase in the thrust force with the increase in the feed rate. In addition, the lowest thrust force achieved with drill 4 (951 N), while the highest thrust force with drill 3 (2418 N). The obtained lowest and highest thrust forces can be attributed to the lowest and highest clearance angles of drill 4 (28°) and drill 3 (12°), respectively. Higher clearance angle leads to decrease in the contact length between the drill cutting edges and newly formed surface in tertiary deformation zone. This, in turn, results in lower friction and easier cutting. From Fig. 6b, it is quite difficult to mention a complete increase or decrease for all the drills in the thrust forces depending on the cutting speed. It is seen that the most important parameter affecting the thrust force is the feed rate [22]. As the feed rate increases, the uncut chip thickness increases [23]. This, in turn, increases the thrust forces.

The effect of the drill geometry, feed rate and cutting speed on the surface roughness is given in Fig. 7. The surface roughness values obtained with drill 2 and drill 3 are close to each other but relatively higher than those obtained with drill 1 and drill 4. At the same time, the lowest surface roughness value (< 1.0 μm) was obtained with drill 4. Increase in the feed rate increases the surface roughness values obtained with drill 1 and drill 4.

Figure 8 gives the effect of drill geometry, feed rate and cutting speed on the deviation on hole diameter. It is seen from the bar graphs that the influence of feed rate is more effective on the deviation on hole diameter than the drill geometry. The lowest deviation on hole diameter is seen for drill 2 at the lowest feed rate of 0.15 mm/rev. This can be explained by the highest split angle of drill 2. Higher split angle enables easy penetration of drill and this, in turn, decrease the deviation on hole diameter. High-split angle also increases self-centering ability of drill especially when drilling work hardening material [22]. On the other hand, the highest deviation on hole diameter is seen for drill 1. This highest value can be attributed to the highest web thickness of drill 1. Increasing web thickness increases the thrust force and the increased thrust force increases the deviation on hole diameter. At relatively high cutting speeds, the deviation on hole diameter increases. Figure 6 a shows that the thrust force is affected by the feed rate, and as the feed rate increases, the thrust forces increase. It is thought that the forces acting on the drill during cutting and these forces affect the deviation values. The web thickness is a predominant factor affecting the torsional rigidity of a drill. However, the chisel edge of a thick web drill needs to be thinned in order to reduce the thrust force [24].

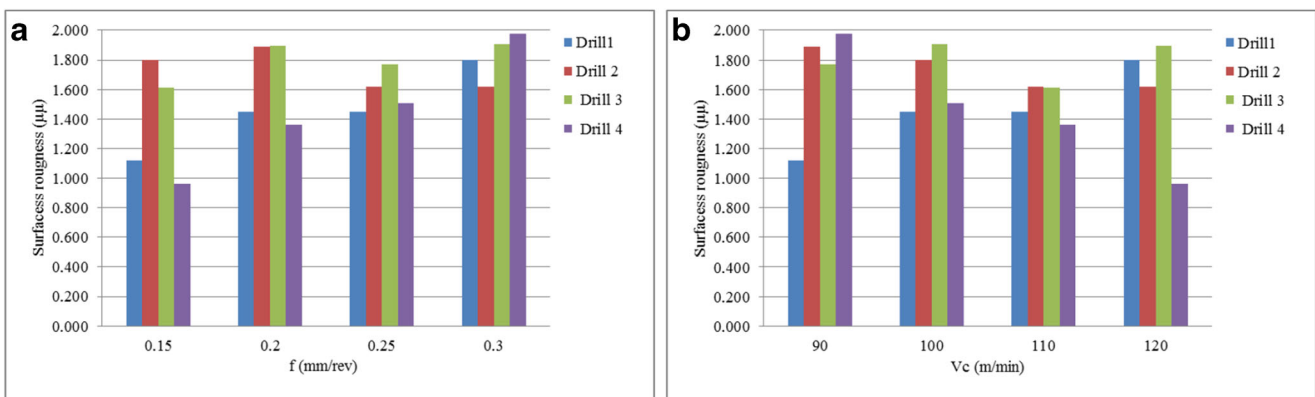
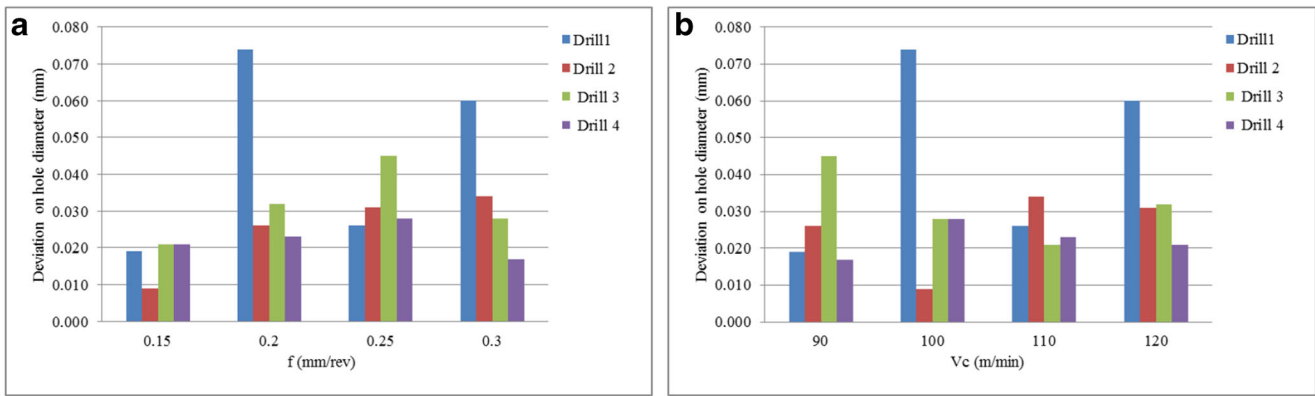


Fig. 7 Effect of a drill geometry-feed rate and b drill geometry-cutting speed interactions on surface roughness



**Fig. 8** Effect of **a** drill geometry-feed rate and **b** drill geometry-cutting speed interactions on deviation of hole diameter

The ratio of the web thickness to the drill diameter directly affects the drill's torsional and bending strength [22].

It is shown in Fig. 9 that the adhering workpiece on the cutting tool is affected by changes in the drill geometry and cutting parameters. The lowest adhering length values are obtained at lower feed rates and drill 4. It is considered decreasing thrust force results in lower adhering workpiece material on the drill.

In this study, the axiomatic design method was used to evaluate the results. Optimum drill geometry, feed rate and cutting speed were determined according to the obtained values of the thrust force, surface roughness, deviation on diameter and length of adhering workpiece. For each functional requirement, the satisfaction degrees and information contents are calculated and according to the information axiom application results listed in Table 5.

The optimum choice that has the lowest information content is alternative test number 13. Based on the obtained results, drill 4, cutting speed of 120 m/min and feed rate of 0.15 mm/rev (A4B1C4) are found to be the optimum cutting conditions. Drill 4 performed best in terms of surface

roughness, deviation on hole diameter, thrust force and adhering workpiece material. This best performance was considered to be the result of its higher clearance angle and low web thickness. Thrust significantly increases with the web thickness and the relief angle, and conversely decreases with the point angle and the helix angle [18].

### 3.2 Wear and length of adhering workpiece on the drill cutting edges

In order to see the wear on the cutting edges of the drills, three drill 4 drills were used at 120 m/min cutting speed and 0.15 mm/rev feed rate with and without cutting fluid. Figure 10 a–c show the stereo microscope images of the drills after drilling 100 holes with and without cutting fluid, after drilling 1500 holes without cutting fluid respectively. In Fig. 10a, there is almost no wear or adhered workpiece material at the cutting edge, chisel edge and margin. As this drill was used with cutting fluid, this is an expected result. When the drilling was carried out without cutting fluid, some adhered workpiece material seen at the cutting edge and slight wear at the chisel edge and margin (Fig. 10b). The drill

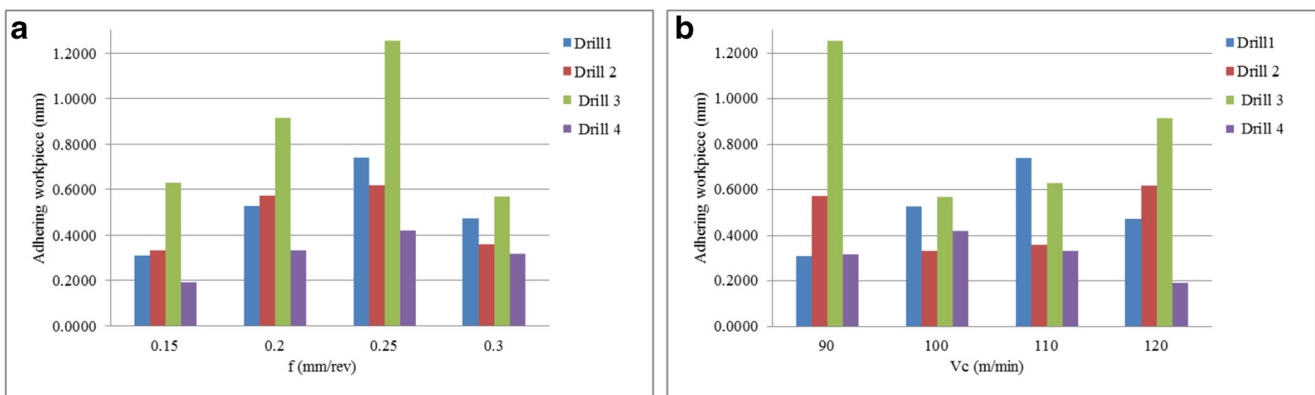


**Fig. 9** The effect of drill geometry and **a** feed rate and **b** cutting speed interactions on the length of adhering workpiece



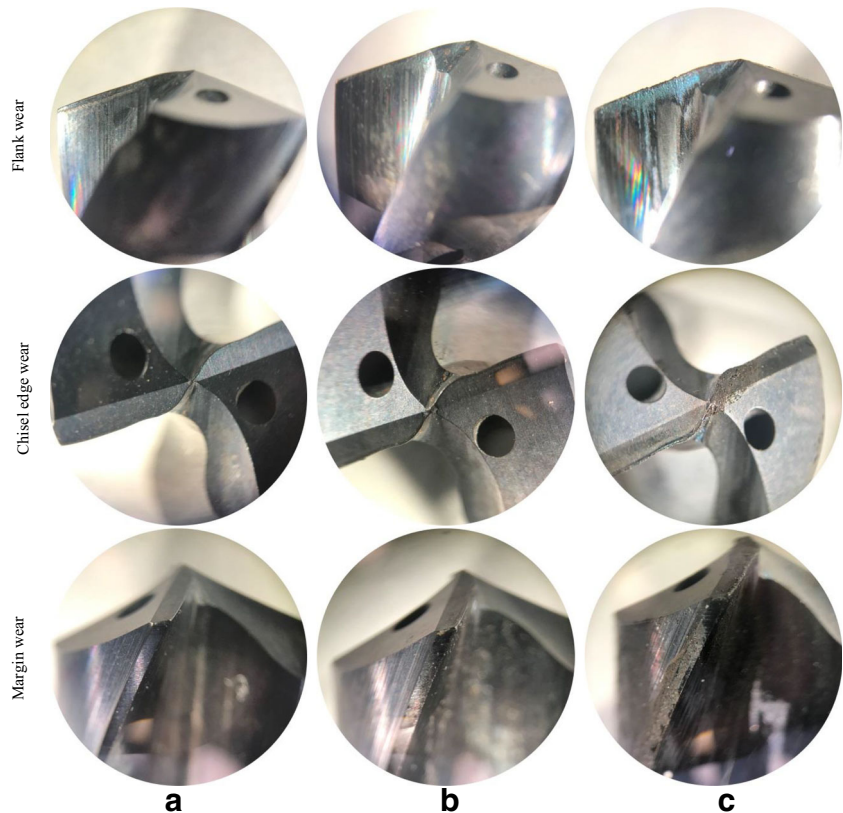
**Table 5** Satisfaction levels (*Ms*) and information content (*I*) for each functional requirements

Test no.	Drill	<i>Ms</i> (Ft)	Thrust force ( <i>I</i> )	<i>Ms</i> (Ra)	Surface roughness ( <i>I</i> )	<i>Ms</i> (D)	Deviation on hole diameter ( <i>I</i> )	<i>Ms</i> (AW)	Adhering workpiece ( <i>I</i> )	$\Sigma I$	Rank
1	Drill 1	0.87	0.02	0.84	0.02	0.85	0.02	0.89	0.01	0.079	2
2	Drill 1	0.69	0.09	0.52	0.23	0.00	1.00	0.68	0.10	1.423	12
3	Drill 1	0.62	0.14	0.52	0.23	0.74	0.07	0.48	0.27	0.705	7
4	Drill 1	0.51	0.24	0.18	0.68	0.22	0.62	0.29	0.50	2.034	14
5	Drill 2	0.93	0.00	0.17	0.68	1.00	0.00	0.87	0.02	0.705	6
6	Drill 2	0.78	0.05	0.09	0.83	0.74	0.07	0.64	0.13	1.080	10
7	Drill 2	0.72	0.08	0.36	0.42	0.66	0.11	0.60	0.16	0.770	8
8	Drill 2	0.61	0.16	0.36	0.42	0.62	0.15	0.50	0.25	0.967	9
9	Drill 3	0.73	0.08	0.36	0.41	0.82	0.03	0.59	0.17	0.689	5
10	Drill 3	0.45	0.30	0.08	0.85	0.65	0.13	0.32	0.46	1.734	13
11	Drill 3	0.16	0.70	0.20	0.64	0.45	0.31	0.00	1.00	2.641	15
12	Drill 3	0.00	1.00	0.07	0.87	0.71	0.09	0.11	0.80	2.753	16
13	Drill 4	1.00	0.00	1.00	0.00	0.82	0.03	1.00	0.00	0.034	1
14	Drill 4	0.89	0.01	0.61	0.16	0.78	0.05	0.87	0.02	0.231	3
15	Drill 4	0.75	0.06	0.46	0.29	0.71	0.09	0.79	0.05	0.485	4
16	Drill 4	0.60	0.16	0.00	1.00	0.88	0.02	0.69	0.10	1.275	11

used to drill 1500 holes without cutting fluid showed significant wear and adhered workpiece material at all the regions (Fig. 10c). In addition, discoloration is also seen at the cutting edge of the drill.

Figure 11 gives the SEM images of the three drill 4 drills. It is also seen from the images that drilling with cutting fluid did result in no adhering workpiece at the chisel edge. This is clearly seen from Fig. 11a. On the other hand, drilling without

**Fig. 10** Wear images of drill 4 **a** after 100 holes using cutting fluid, **b** after 100 holes without using cutting fluid and **c** after 1500 holes without using cutting fluid



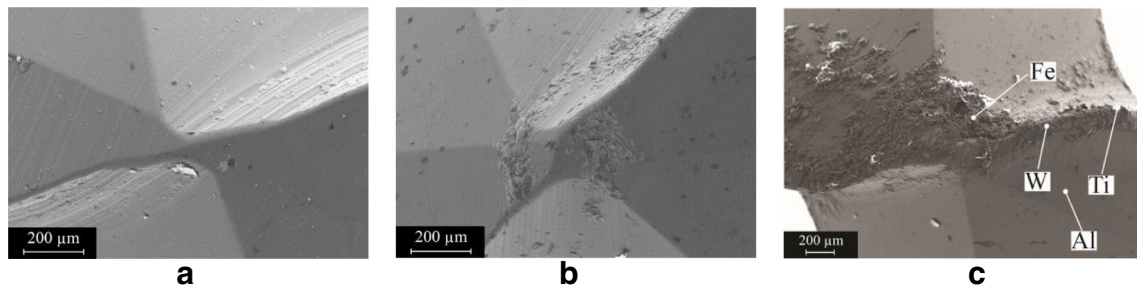


**Fig. 11** SEM images of drill 4 **a** after 100 holes using cutting fluid, **b** after 100 holes without using cutting fluid and **c** after 1500 holes without using cutting fluid

cutting fluid led to some adhered material and increasing number of holes up to 1500 significantly increased the amount of adhered workpiece material (Fig. 11b, c).

The adhered workpiece on the drills is most likely to be over the worn areas of the drills. Therefore, it was decided to measure the width of the adhered workpiece at the chisel edges as an indirect indication of the wear. Figure 12 shows the width of the adhered workpiece for the drills used to drill 100 holes with and without cutting fluid. Figure 12 shows that increasing number of holes increases the width of adhered workpiece for the both drills. When compared with the one

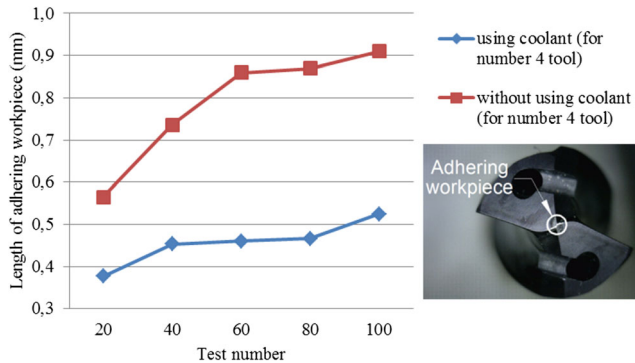


**Fig. 12** Width of adhered workpiece material at the cutting edges of drill 4

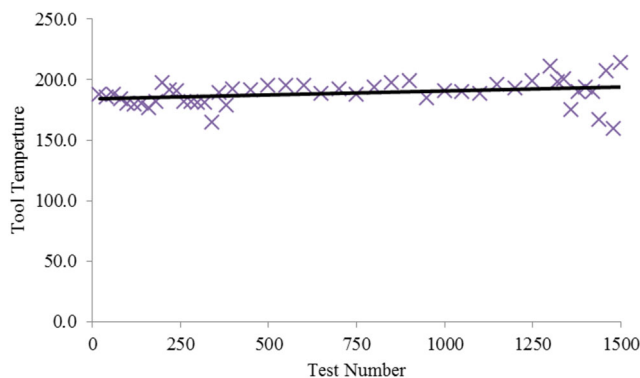


**Fig. 13** Drill temperature

used with cutting fluid, the drill used without cutting fluid experiences significant amount of deposits of workpiece material. This clearly shows the influence of the cutting fluid.

When the SEM images in Fig. 11a, b are examined, no abrasion or adhesion is seen on the drill used with cutting fluid while adhesion of workpiece materials is seen on the drill used without cutting fluid. After drilling 1500 holes, the amount of adhered workpiece materials significantly increases.

During the drilling tests up to 1500 holes, temperatures of the drill and surface roughness values of the holes were measured. Figure 13 shows the drill temperature values while Fig. 14 shows the surface roughness values. Although a slight increase is seen in the temperature values with increasing number of the holes, the temperature values do not scatter much up to about 1250 holes. Beyond 1250 holes, a relatively large scatter in the temperature values are seen. On the other hand, the surface roughness value also increase slightly with increasing number of the holes and vary significantly in the range about 2 and 4 μm.

### 4 Conclusions

In this study, for the multiple performance characteristics (thrust force, surface roughness, deviation on hole diameter and length of adhering workpiece), the optimum tool geometry and cutting parameters were determined through the axiomatic design method. For this purpose, drilling tests on

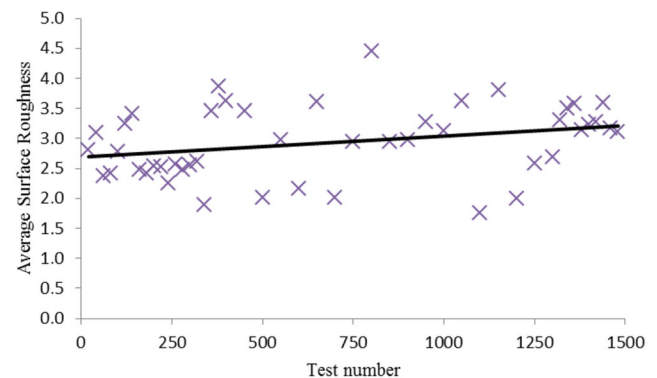


**Fig. 14** Average surface roughness

GGG50 workpiece were carried out using four different drill geometries and at various cutting speeds and feed rates. The following conclusions can be drawn from the present study:

- The angles that make up the drill geometry and cutting parameters greatly affect the drilling performance.
- According to the axiomatic design method, drill 4 was found to be the optimum drill geometry and 0.115 mm/rev feed rate and 120 m/min cutting speed the optimum drilling parameters.
- Drill 4 performed best in terms of surface roughness, deviation on hole diameter, thrust force and adhering workpiece material. This best performance was considered to be the result of its highest clearance angle and low web thickness.
- In drilling with and without cutting fluid, no significant wear was observed on the drills after 100 holes, adhesion of workpiece material occurred and the amount of adhesion was doubled when the cutting fluid was not used. After 1500 holes, the amount of adhesion increased significantly.

**Acknowledgements** The authors would like to thank KARCAN for its contributions to the study.

**Funding information** The authors would like to thank TUBITAK, TR, for supporting this study through project 3130691 as part of the ‘TUBITAK 1501 – Industrial R&D Project Funding Program’.

**Nomenclature** AD, axiomatic design; BH, Brinell hardness; f, feed rate (mm/rev); FR, functional requirement; Ft, thrust force; GGG50, spheroidal graphite cast iron; JC, Johnson cook; SEM, scanning electron microscopy; Ra, average surface roughness ( $\mu\text{m}$ ); Vc, cutting speed (m/min)

## References

1. Groover MP (2010) Fundamentals of modern manufacturing, materials, processes, and systems, 4th, John Wiley & Son
2. Kalpakjian S, Schmid SR (2009) Manufacturing engineering and technology, 8th, Prentice Hall
3. Abele E, Fujara M (2010) Simulation-based twist drill design and geometry optimization. CIRP Ann Manuf Technol 59:145–150
4. Kivak T, Seker U (2015) Effect of cryogenic treatment applied to M42 HSS drills on the machinability of Ti-6Al4V alloy. Mater Technol 49:949–956
5. Tsai WD, Wu SM (1979) A mathematical model for drill point design and grinding. J Eng Ind 101:333–340
6. Tsai WD, Wu SM (1979) Computer analysis of drill point geometry. Int J Mach Tool Des Res 19:95–108
7. Chen WC, Fuh KH, Wu CF, Chang BR (1996) Design optimization of a split-point drill by force analysis. J Mater Process Technol 58: 314–322
8. Ren K, Ni J (1999) Analyses of drill flute and cutting angles. Int J Adv Manuf Technol 15:546–553
9. Paul A, Kapoor SG, DeVor RE (2005) Chisel edge and cutting lip shape optimization for improved twist drill point design. Int J Mach Tools Manuf 45:421–431
10. Hsieh JF (2005) Mathematical model for helical drill point. Int J Mach Tools Manuf 45:967–977
11. Pirtini M, Lazoglu I (2005) Forces and hole quality in drilling. Int J Mach Tools Manuf 45:1271–1281
12. Degenhardt JA, DeVor RE, Kapoor SG (2005) Generalized groove-type chip breaker effects on drilling for different drill diameters and flute shapes. Int J Mach Tools Manuf 45:1588–1597
13. Audy J (2008) A study of computer-assisted analysis of effects of drill geometry and surface coating on forces and power in drilling. J Mater Process Technol 204:130–138
14. Audy J (2008) A study of computer assisted analysis of effects of drill point geometrical features on forces and power in drilling with general purpose twist drills. MM Sci J 1:5–8
15. Wang J, Zhang Q (2008) A study of high-performance plane rake faced twist drills. Part I: Geometrical analysis and experimental investigation. Int J Mach Tools Manuf 48-11:1276–1285
16. Wang J, Zhang Q (2008) A study of high-performance plane rake faced twist drills. Part II: Predictive force models. Int J Mach Tools Manuf 48-11:1286–1295
17. Sambhav K, Dhande SG, Tandon P (2010) CAD based mechanistic modeling of forces for generic drill point geometry. Comput Aided Des Appl 7:809–819
18. Ema S (2012) Effects of twist drill point geometry on torque and thrust. Sci Rep Fac Educ Gifu Univ 36:165–174
19. Chatterjee S, Mahapatra SS, Abhishek K (2016) Simulation and optimization of machining parameters in drilling of titanium alloys. Simul Model Pract Theory 62:31–48
20. Kılınç, B (2009) The effect of copper addition on mechanical properties of GGG50 grade cast iron, MSc Thesis, Istanbul University
21. Tarcan E (2012) An axiomatic design approach to multi-objective optimization. MSc Thesis, Marmara University
22. Lazar, M (2012) Cutting force modelling for drilling of fiber-reinforced composites. PhD Thesis, École Polytechnique Fédérale De Lausanne University
23. Çiftçi İ, Gökçe H (2019) Optimisation of cutting tool and cutting parameters in machining of molybdenum alloys through the Taguchi method. J Fac Eng Archit Gazi Univ 34(1):201–213
24. Fuh KH, Chen WC (1995) Cutting performance of thick web drills with curved primary cutting edges. Int J Mach Tools Manuf 35(7): 975–991

**Publisher's note** Springer Nature remains neutral with regard to jurisdictional claims in published maps and institutional affiliations.